Heliyon 10 (2024) e22944

Contents lists available at ScienceDirect

Heliyon

journal homepage: www.cell.com/heliyon

Identification of the role of pyroptosis-related genes in chronic rhinosinusitis based on WGCNA

Yarui Wan [a], Yanfei Wang [b], Sheng Xu [a], Hui Du [a], Zhiqi Liu [a,*]

[a] Department of Otolaryngology, Hubei Maternal and Child Health Hospital, Hubei, 430070, PR China
[b] Department of Otolaryngology, Beijing Chaoyang Hospital Affiliated to Capital Medical University, Beijing, 100020, PR China

ARTICLE INFO

Keywords:
Chronic rhinosinusitis
Pyroptosis
WGCNA
PPI
Hub gene

ABSTRACT

Background: Chronic rhinosinusitis (CRS) is a complex chronic inflammatory disease of the nose, paranasal sinus, and upper respiratory tract. Its treatment methods mainly include antibiotic treatment and surgical treatment. However, the molecular mechanism of its inflammation is still unclear. Pyroptosis is a programmed cell death. As an important natural immune response, pyroptosis plays an essential role in fighting infection.

Methods: In this paper, a weighted co-expression network (WGCNA) was used to screen gene modules significantly related to CRS. Then it intersects with the genes related to scorching death (PRGs). We evaluated the immune landscape of CRS by the expression of intersecting genes. In addition, in the enrichment analysis of intersection genes and PPI network analysis, we verified the pathways closely related to CRS and hub genes. Finally, the interaction network between the hub gene, miRNA, and TF was constructed. In this paper, qRT-qPCR technology was also used to detect the hub gene related to CRS.

Results: Hub genes (CASP3, IL18, NAIP, NLRC4, and TP53) found in this paper are directly or indirectly related to CRS, and these genes were proved to be of diagnostic significance to CRS by ROC curve and qRT-qPCR vertification. In the infiltration abundance of CRS and its control group, the infiltration abundance of Plasma cells, T cells follicular helper, Macrophages M2, Dendritic cells activated, and Neutrophils cells in the two groups were significantly different. We also constructed the interaction network between the hub genes and miRNAs and the interaction network between hub genes and TFs. Most of these miRNAs and TFs were also related to CRS.

Conclusions: With the help of the WGCNA and PPI analysis, our results provide a better understanding of the role of biomarkers CASP3, IL18, NAIP, NLRC4, and TP53 in the development of CRS and provide a research basis for the mining of biomarkers related to the diagnosis and treatment of CRS.

1. Introduction

Chronic rhinosinusitis (CRS) is a common disease in otorhinolaryngology, and its symptoms are a stuffy nose, runny nose, and dysosmia [1]. The main treatment methods include antibiotic therapy and surgical treatment. However, CRS has a high recurrence rate. In addition, previous studies have confirmed that the immune disorder caused by the destruction of the nasal sinus epithelial barrier plays a crucial role in CRS [2]. However, its related molecular mechanism is still unclear. Therefore, it is urgent to study its

* Corresponding author.
E-mail address: liuwu188@sina.com (Z. Liu).

https://doi.org/10.1016/j.heliyon.2023.e22944
Received 11 August 2023; Received in revised form 20 November 2023; Accepted 22 November 2023
Available online 27 November 2023

Table 1
qRT-qPCR reaction system.

Composition	Volume
2 × SYBR Premix Ex Taq	10.0 μL
Fwd Primer (5 pmol/μL)	2.0 μL
Reverse Primer (5 pmol/μL)	2.0 μL
Template (RT product cDNA)	2.0 μL
dd H_2O	4.0 μL

Note: The circulating temperature is: 95 °C 30 s, 95 °C 15 s, 60 °C 30 s, 40 cycles.

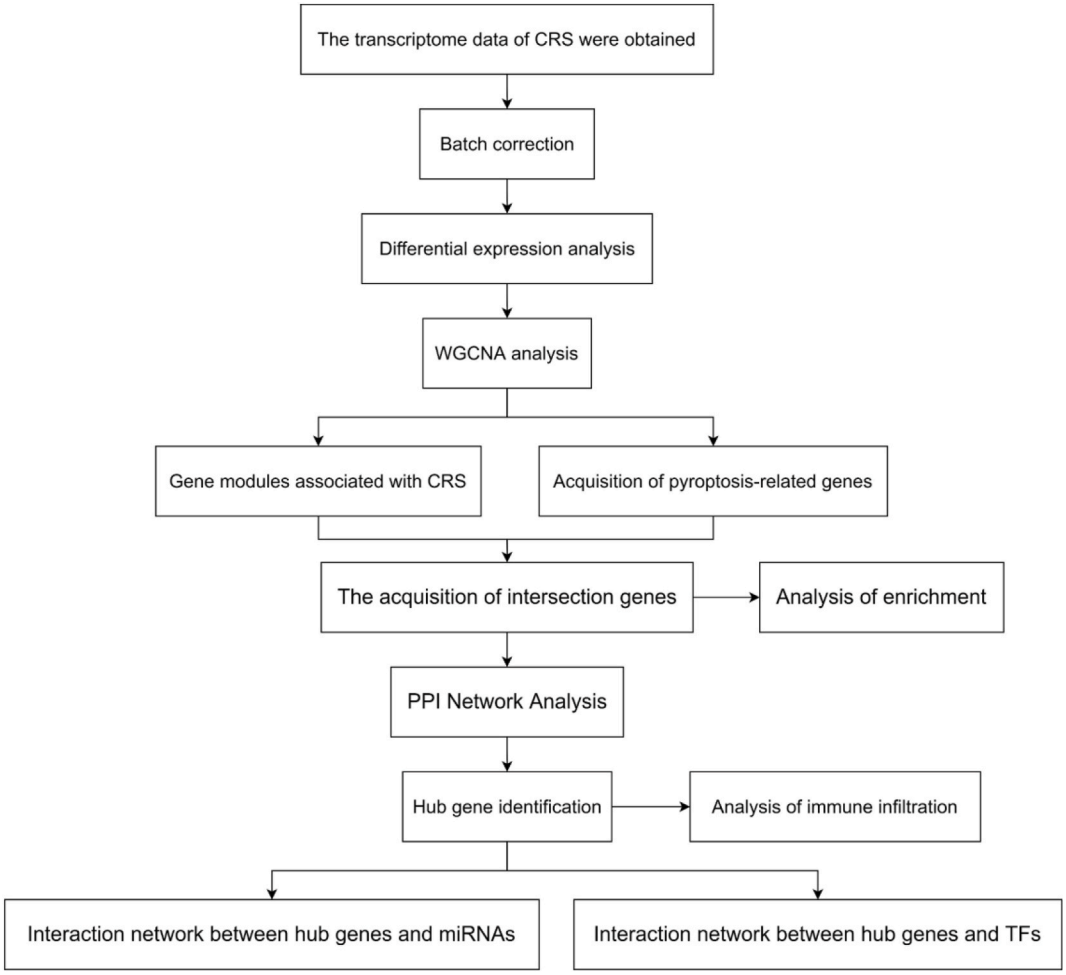

Fig. 1. The technical flow chart.

pathogenesis at the molecular level and assist in the development of new drugs.

As a kind of programmed cell death, pyroptosis has been proven to be closely related to diseases such as inflammation and tumor [3, 4]. The process of pyroptosis can be roughly described as follows: because it mediates a variety of caspases through the activation of inflammatory corpuscles, the cells continue to extend until they rupture and die. This process leads to the release of cellular substances, which leads to an inflammatory reaction [5]. However, the role of pyroptosis in CRS, a chronic inflammation, is still unclear.

Based on the transcriptome data of CRS, this paper aimed to explore the important role of pyroptosis-related genes (PRGs) in the occurrence and development of CRS. Specifically, we downloaded the transcriptome data of CRS and its control group from the GEO database (https://www.ncbi.nlm.nih.gov/geo/). After batch correction and differential expression analysis, we used the weighted co-expression network (WGCNA) algorithm to screen gene modules related to CRS. After crossing the gene module and the genes related to scorch death, the enrichment analysis and protein interaction (PPI) network analysis of the intersection genes were carried out. Three algorithms of network analysis were used to identify the hub gene in the PPI network, and external data sets were used to verify

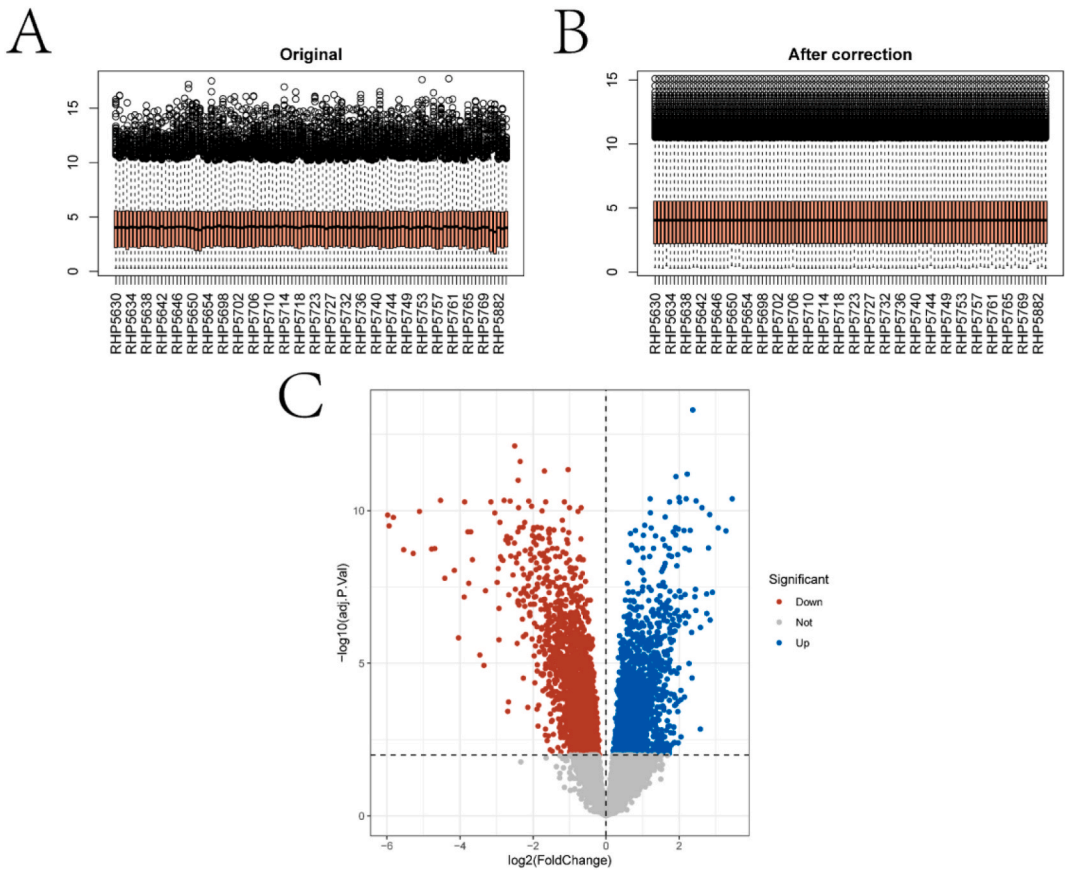

Fig. 2. Box diagram and differential expression analysis of transcriptome data before and after correction. A and B are box charts before and after the transcription data calibration. C is the volcano map obtained by differential expression analysis of transcriptome data.

ROC. In addition, based on Cibersort analysis of hub gene expression, this paper explored the difference in infiltration abundance of 22 kinds of immune cells in CRS and its control group. Finally, through the interaction network of hub gene, miRNA, and transcription factor (TF), we found miRNA and TF related to CRS. This study aimed to identify potential PRGs with diagnostic value for CRS to provide possible therapeutic approaches for CRS patients.

2. Method

2.1. Data acquisition and batch correction

Transcriptome data of CRS and its control group were obtained from the GEO database. Among them, GSE136825 was used as the training data set (including 42 CRS samples and 33 control samples), and the platform is GPL20301 Illumina His EQ 4000 (*Homo sapiens*). GSE179265 was utilized as the external test data set (including 9 CRS samples and 7 control samples), and the platform is GPL24676 Illumina NovaSeq 6000 (*Homo sapiens*). GSE36830 was utilized as another external test data set (including 18 CRS samples and 6 control samples), and the platform is GPL570 [HG-U133_Plus_2] Affymetrix Human Genome U133 Plus 2.0 Array (*Homo sapiens*). R-package "SVA" was applied to remove the batch effect of samples.

2.2. Differential expression analysis

In the study, DEGs extraction of training set data was realized by using the R-packet "limma." DEGs with $|\log FC|>0$ and adj.P.Val<0.01 was finally retained.

2.3. Weighted correlation network analysis

We used the R package "WGCNA" to implement the WGCNA algorithm, which is applied to screen gene modules significantly related to CRS. Specifically, we imported DEGs and sample labels into the WGCNA package for analysis. The minimum number of modules was 50, and the optimal power value was 8. In this method, the weighted adjacency matrix provided by the network was

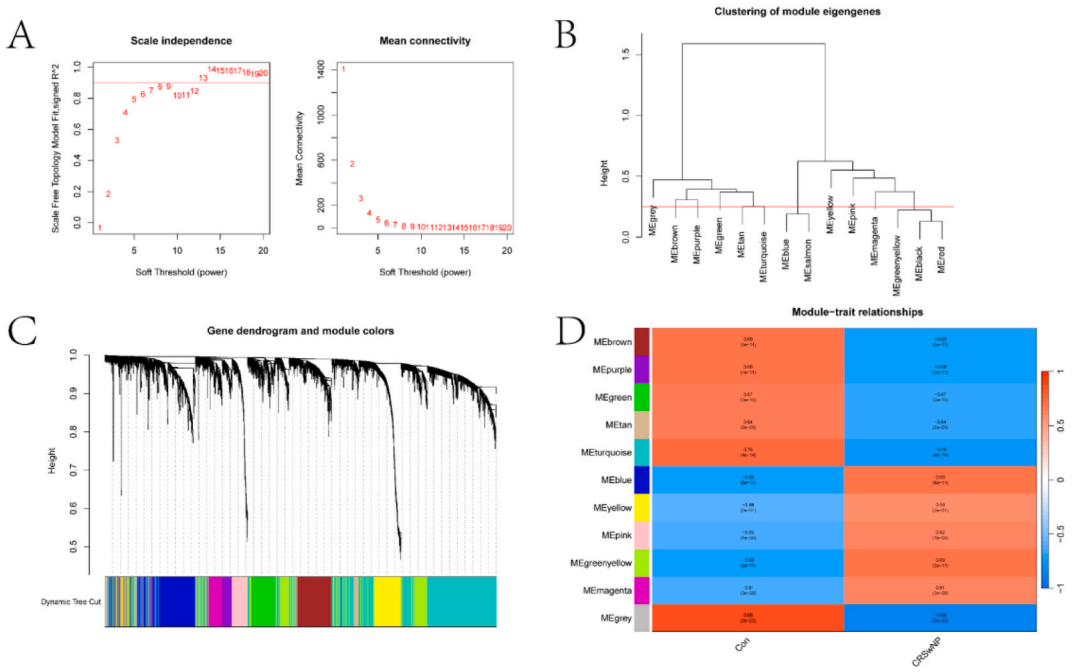

Fig. 3. WGCNA analysis of differential genes. A is the graph of scale independence, average connectivity, and scale-free topology. B is cluster plot analysis of the relationship between CRS and modules. C and D give the cluster tree diagram of co-expression network modules and the correlation between different gene modules and CRS.

transformed into an overlapping topological matrix (TOM). The cluster tree structure of TOM was constructed by hierarchical clustering. In addition, according to the gene expression pattern, the gene was divided into multiple modules, and then the correlation and significance between each module and CRS were calculated.

2.4. GO and KEGG enrichment analysis

With the R-packet "clusterprofile," the KEGG and GO enrichment analysis of the genes in the gene module with a significant positive relationship to CRS was performed. The R tool "ggplot2″ was then implemented to visualize the outcomes of the enrichment analysis.

2.5. PPI network construction and hub genes identification

The String database (http://string.embl.de/) was utilized in this work to import the gene modules with significantly positive CRS correlation. The confidence level was adjusted to 0.4, and the PPI network findings were obtained. Then, the network was displayed using the Cytoscape software. The hub gene in the network was identified via using three algorithms: Betweenness, Degree and MCC provided by cytoscape plug-in.

2.6. Immune landscape exploration based on the CIBERSORT algorithm

In this paper, the expression of the hub gene in CRS and its control group was introduced into the CIBERSORT algorithm, and the difference of infiltration abundance of 22 kinds of immune cells between the two groups was evaluated.

2.7. Construction of interaction network between hub genes, miRNA, and TF

For the construction of the interactive network between the hub gene and miRNA, this paper was based on the TarBase v8.0 database of the networkanalyst database (https://www.networkanalyst.ca).

The ENCODE database.

(http://amp.pharm.mssm.edu/harmonizome/dataset/encode%20+%20transcription%20+%20factor%20+%20targets) was applied to create the interaction network between the hub gene and TF.

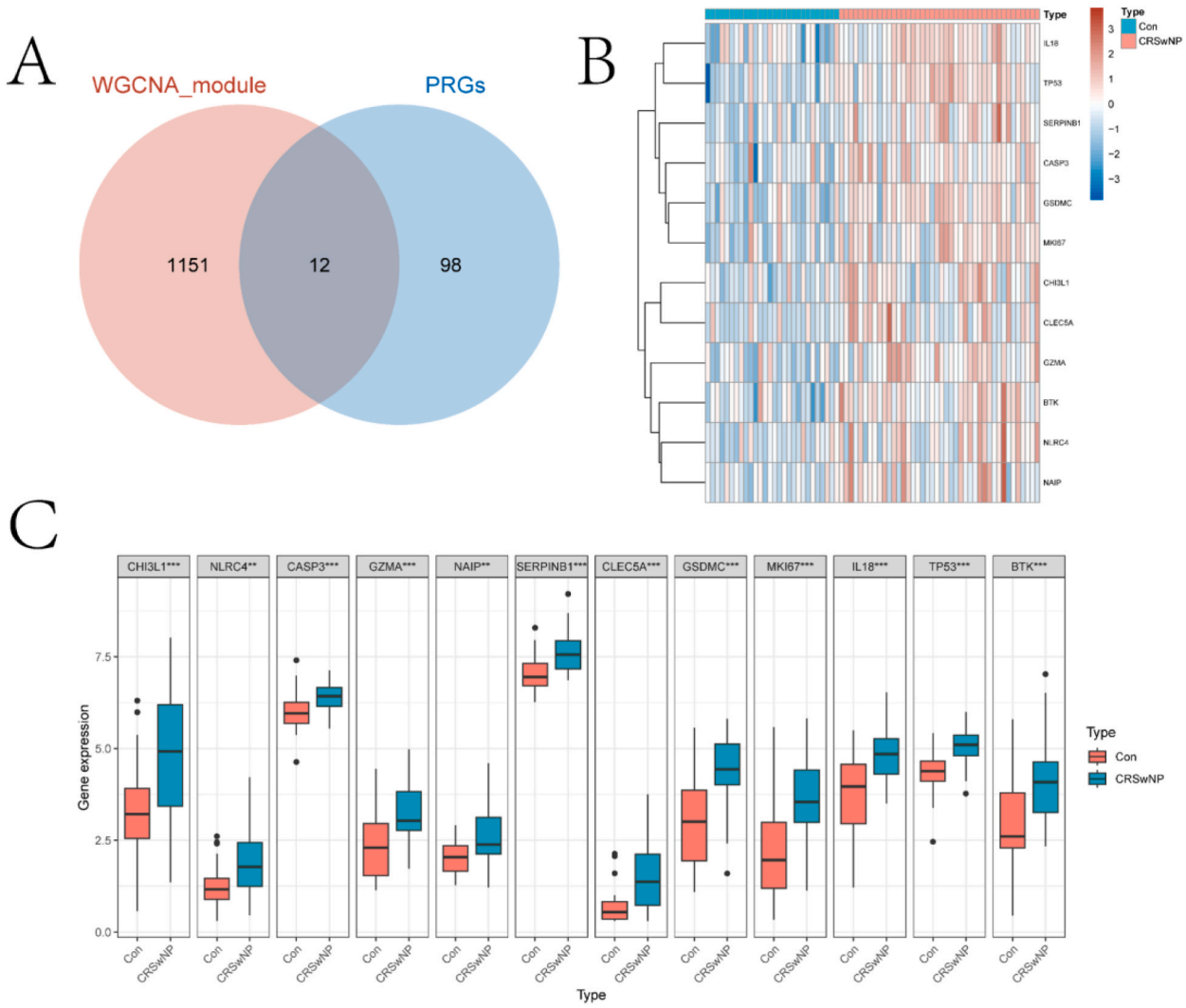

Fig. 4. Acquisition and expression analysis of intersection gene. A is the Wayne diagram of the intersection of genes and PRGs in the significant correlation module. B and C are the heat map and box map of intersection gene expression in CRS and its control group, respectively.

2.8. qRT-qPCR experimental verification

In this paper, qCPR experiment verified that the mRNA expression level of hub genes was screened in two groups (normal control group (NC) and CRS group). The CRS group used cells from CRS with nasal polyps (CRSwNP) samples. Specifically, the cells used were the nasal mucosal epithelial celcls of CRSwNP patients and normal human nasal mucosal epithelial cells. After RNA extraction from cells, cDNA preparation by RT, and mRNA amplification by fluorescence quantitative qRT-qPCR, data processing and analysis were carried out, and histogram was drawn. The primer sequence and quantitative PCR reaction system (Table 1) are shown below.

Primer sequence:

NLRC4: F-5′-TGTGTGACCTTGCCCAGAAC-3′
R-5′-TGGACTTGCCTTTGCCAGAT-3′
TP53: F-5′-TGAGGAGTGTCCGAAGAGAATG-3′
R-5′-GGAAGGCAGTCTGGCTGATA-3′
CASP3: F-5′-GCTCATACCTGTGGCTGTGT-3′
R-5′-GCTTTGGTTCCCGCAAAACT-3′
NAIP: F-5′-ACCCCTATGTGCTTGAGTTTCC-3′
R-5′-GAATCCCAGACGAAGTCCCC-3′
GAPDH: F-5′-TCAGCAATGCCTCCTGCAC-3′
R-5′-TCTGGGTGGCAGTGATGGC-3′

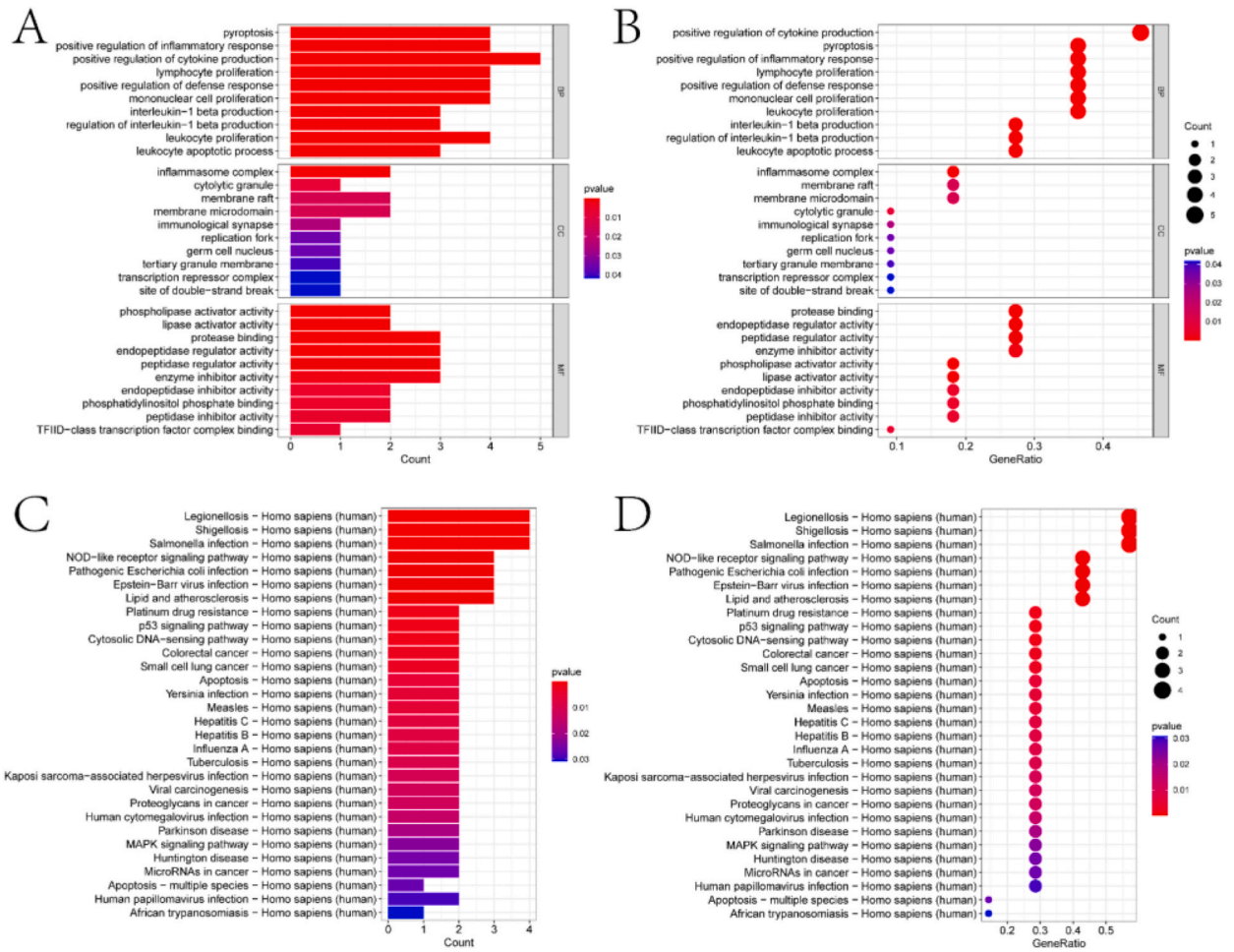

Fig. 5. Enrichment analysis of intersection genes. A and B give the histogram and bubble chart of GO enrichment analysis of the intersection gene, respectively. C and D provided the histogram and bubble diagram of the KEGG enrichment analysis of the intersection gene, respectively.

3. Results

3.1. Data acquisition and batch correction

Fig. 1 shows the technical flow chart. In this study, the training set data was batch-corrected. Fig. 2A–B displays the box charts of the data set before and after rectification. This researcher conducted a differential expression analysis on the corrected data. The volcanic map produced by the differential expression analysis procedure was illustrate in Fig. 2C.

3.2. Screening CRS-related modules based on the WGCNA algorithm

Further, DEGs were input into the WGCNA algorithm. The algorithm calculated the coexpression correlation coefficient between genes according to the expression level of DEGs and then clustered the genes based on Euclidean distance and pruned them. Fig. 3A show the trimmed gene cluster tree output by the algorithm. Moreover, Fig. 3B demonstrate the connection between different gene modules and CRS. Among them, the blue module and green-yellow module had the highest correlation with CRS (Fig. 3C–D). Therefore, we will further analyze the genes in the blue module and the green-yellow module.

3.3. Enrichment analysis and PPI network construction

In this paper, the genes in the significant gene module were intersected with PRGs, and 12 intersected genes were obtained (Fig. 4A). We analyzed the expression calorimetry (Fig. 4B) and expression difference box diagram (Fig. 4C) of 12 intersecting genes in CRS and its control group. Fig. 5 showed the structure of the enrichment analysis of intersection genes in this paper. Fig. 5A–B and Fig. 5C–D showed the histogram and bubble diagram of the intersection gene GO enriched by KEGG, respectively. For the significant

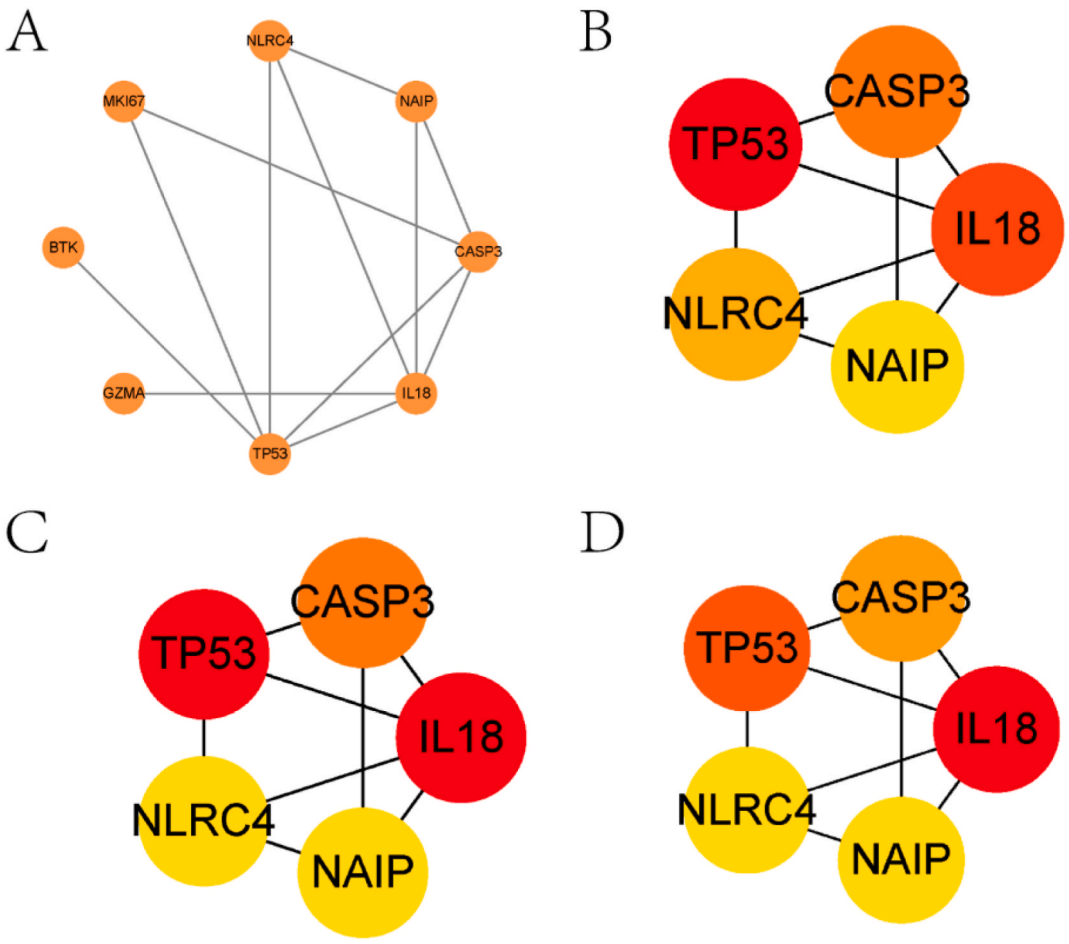

Fig. 6. PPI network analysis and hub gene identification of intersection genes. A is a PPI network constructed by intersecting genes. B-D give the results to screen hub genes in cytoscape by three algorithms (Betweenness, Degree, and MCC), respectively.

pathways obtained by enrichment analysis, this paper will discuss them in detail in the fourth section. In addition, we also analyzed the PPI of the intersecting genes and got the PPI network (Fig. 6A). Fig. 6B–D are hub genes in the network identified based on three algorithms of Betweeness, Degree, and MCC in cytoscape. We intersected the genes selected by the three algorithms, and finally got five hub genes (CASP3, IL18, NAIP, NLRC4, and TP53).

We used both internal and external data sets to confirm the expression levels of these five genes. The ROC curves for five genes from the internal data set can be seen in Fig. 7A–E. Fig. 8A shows the expression differences of five genes between the CRS group and control group on the external test set. The ROC curves for five genes on external data sets were displayed in Fig. 8B–F. The ROC curves for five genes on another external data sets were displayed in Fig. 8G–K. The AUC of all five genes was greater than 0.6, which was of diagnostic significance for CRS. Finally, the nomogram model of diagnostic genes was constructed (Fig. 9A). Fig. 9B–C shows the calibration curve and decision curve of nomogram model respectively. As can be seen from the figure, the nomogram model jv has high diagnostic performance.

3.4. Immune landscape of intersecting genes

In this research, the expression levels of five hub genes in CRS and its control group were introduced into the CIBERSORT algorithm, the infiltration abundance of 22 kinds of immune cells in the two groups was obtained, and the box diagram of Fig. 10A was drawn. Among them, the infiltration abundance of Plasma cells, T cells follicular helper, Macrophages M2, Dendritic cells activated, and Neutrophils was significantly different between the two groups. We will analyze in detail the critical role of these immune cells in the development of CRS inflammation in the discussion section.

Besides, we also examined the correlation between five hub genes and immune cells (Fig. 10B–F). Among them, CASP3 was significantly related to Dendritic cells activated, T cells follicular helper, Macrophages M2, and Mast cells resting. IL-18 was markedly correlated with NK cells resting and Plasma cells. NAIP was notably relevant to Macrophages M2 and Plasma cells. NLRC4 was dramatically associated with Neutrophils, Macrophages M2, T cells CD4 memory activated and Plasma cells. TP53 had a obviously

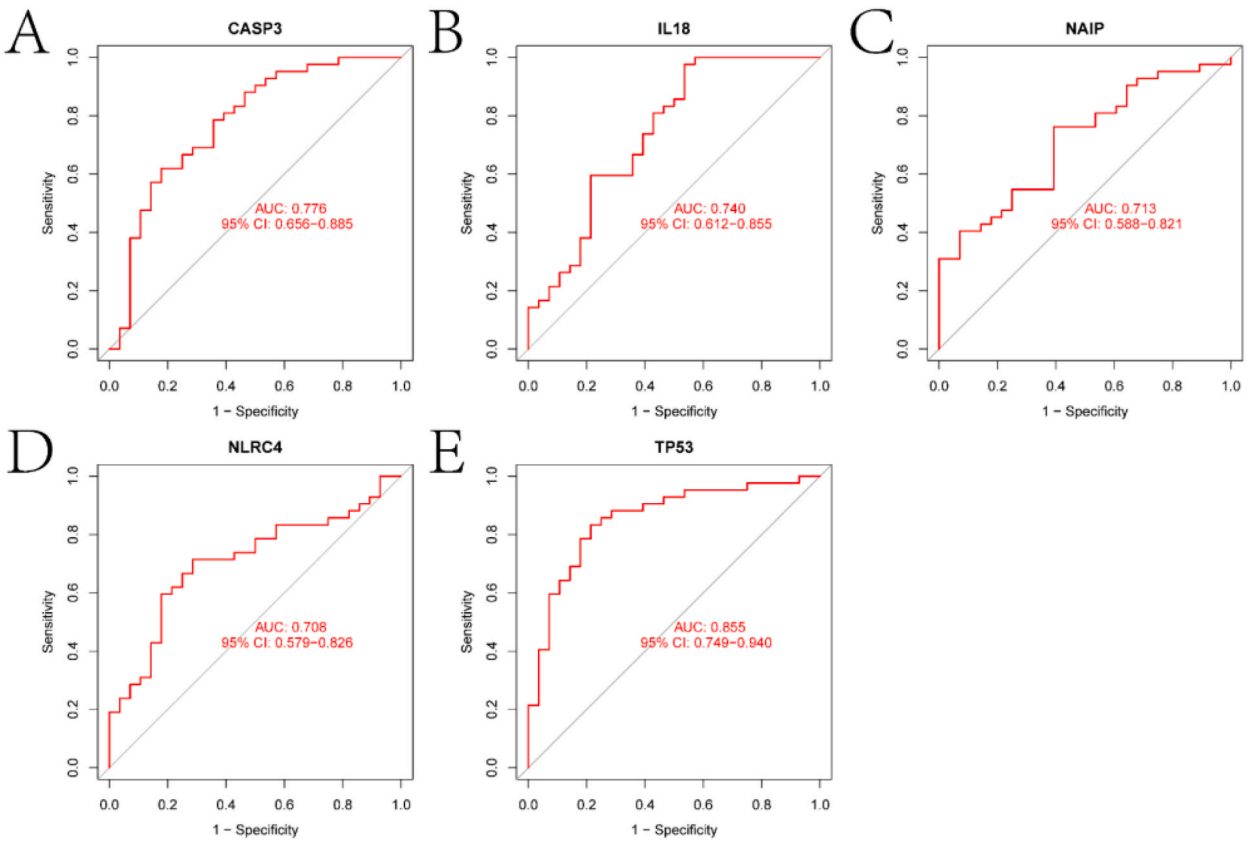

Fig. 7. ROC verification of hub gene in internal data set. A-D are ROC curves of CASP3, IL18, NAIP, NLRC4, and TP53 in the GSE136825 data set, respectively.

relationship with T cells follicular helper, Dendritic cells activated, and Plasma cells.

3.5. Interaction network between hub genes, miRNA, and TF

This paper discussed miRNA interacting with five hub genes based on the TarBase database (v0.8) (Fig. 11A). Among them, CASP3, TP53, and IL18 have interactions with many miRNAs. In addition, TF interacting with five hub genes was displayed based on the JASPAR database (Fig. 11B). Among them, CASP3, TP53, NAIP, NLRC4, and IL18 have interactions with many TFs. We will discuss these miRNA and TF in the discussion section.

3.6. qRT-qPCR experimental verification results

The nasal mucosal epithelial cells of CRSwNP patients and normal human nasal mucosal epithelial cells were evaluated by qRT-qPCR to verify whether NLRC4, TP53, CASP3 and NAIP were differentially expressed in the samples. It was found that TP53 and CASP3 had elevated expression in the CRSwNP group as compared with the expression levels in the control group (Fig. 12).

4. Discussion

CRS is an otolaryngology disease with a high recurrence rate. Pyroptosis is a kind of programmed cell death, which is closely related to the inflammatory reaction of many diseases. In this paper, the role of pyroptosis -related genes in CRS was discussed, but it was not clear. Therefore, this paper analyzed the different expressions of the training set data after batch correction.

Firstly, the WGCNA algorithm was used to screen the modules related to CRS. The DEGs were imported into the WGCNA package for analysis, and the gene module related to CRS was screened. Then the genes in the gene module were intersected with PRGs collected in previous literature. GO and KEGG enrichment analyses were performed on the intersecting genes (Fig. 5). In the GO enrichment pathway, we determined that pyroptosis had closed relatedness to infection [6]. IL-17A can induce the focal death of human nasal epithelial cells (hNEC) in patients with CRSwNP through extracellular signal-regulated kinase (ERK) pathway [7]. NLRP3 is closely related to inflammation, and it has been confirmed that NLRP3 is involved in the pathogenesis of CRS [8]. S100A8 is a calcium and zinc binding protein that plays an important role in regulating inflammatory processes and immune response. Nakatani A

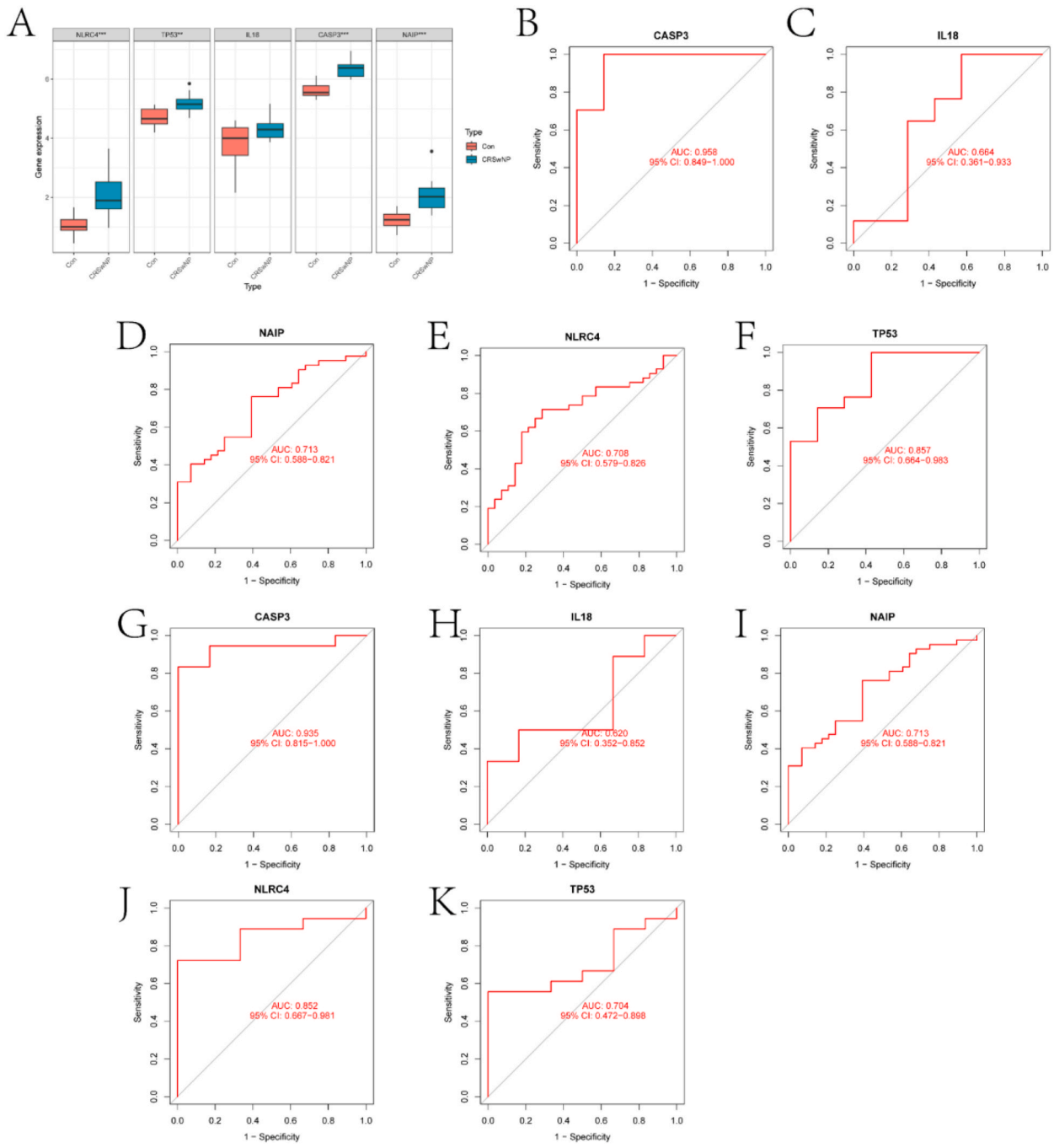

Fig. 8. ROC verification of hub gene in external data set. A is the expression box diagram of the hub genes in CRS and its control group. B–F are ROC curves of CASP3, IL18, NAIP, NLRC4, and TP53 in the GSE179265 data set, respectively. G-K are ROC curves of CASP3, IL18, NAIP, NLRC4, and TP53 in the GSE36830 data set, respectively.

et al. confirmed that S100A8 could induce the production of interleukin -1β in the nasal epithelium, which is involved in the pathogenesis of eosinophilic rhinosinusitis [9]. In the KEGG enrichment pathway, Ding S et al. certained that the NOD-like receptor signaling pathway is a critical CRS signaling pathway through network pharmacological analysis [10]. There are differences in the expression of key apoptosis markers at mRNA and miRNA levels in patients with CSRwNP [11]. Apigenin can alleviate the nasal mucosa remodeling induced by TGF-β1 by inhibiting the MAPK/NF-kB signaling pathway of CRS, which indicates that apigenin can be used as a potential therapeutic drug for CRS [12].

Second, we used the PPI network to identify hub genes for CRS from intersection genes. Specifically, based on three algorithms, we

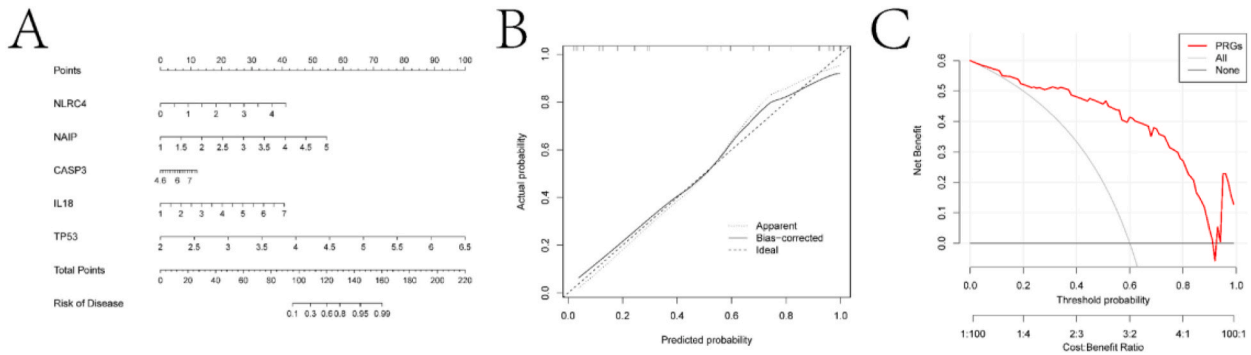

Fig. 9. Nomogram model of diagnostic genes. A is the nomogram model of diagnostic gene. B is the calibration curve of nomogram model. C is the decision curve of nomogram model.

screened hub genes (CASP3, IL18, NAIP, NLRC4, and TP53). The protein encoded by CASP3 gene is a cysteine-aspartic protease, which is involved in the signal pathway of apoptosis and inflammation. The two pathways are all associated with CRS [8,11]. CRS is characterized by persistent symptomatic inflammation of nasal and sinus mucosa [13]. IL-9 plays an important role in triggering an inflammatory reaction, stimulating cell proliferation, and preventing cell apoptosis by binding with the IL-9 receptor (IL-9R). They are overexpressed at protein and mRNA levels in CRS [14]. IL-18 has been proven to be a potential therapeutic target for CRS [15]. The protein encoded by NAIP gene can inhibit cell apoptosis induced by various signals. Specifically, it is an anti-apoptosis protein that inhibits the activities of CASP3, CASP7, and CASP9. NLRC4 encodes a member of the NLR family containing a caspase recruitment domain and is also a key component of inflammatory corpuscles [16]. TP53 can induce cell cycle arrest, apoptosis, aging, DNA repair, or metabolic changes. Huang GJ et al. identified TP53 as an important DEFGs of CRSwNP [17]. We also verified the ROC curves of the hub genes. The AUC of these genes in the training set and the test set was greater than 0.5, which was of diagnostic significance for CRS.

Thirdly, based on the expression of hub genes, we evaluated the infiltration abundance of 22 kinds of immune cells in CRS and its control group. Among them, the infiltration abundance of Plasma cells, T cells follicular helper, Macrophages M2, Dendritic cells activated, and Neutrophils cells in the two groups were significantly different. The relationship between these immune cells and CRS can be confirmed in the following literature. Arjun Mandih et al. used CD27 as a marker of plasma cells and confirmed through experiments that the existence of biofilm in CRS seems to be related to the host inflammatory reaction caused by plasma cells [18]. T cells follicular helper and their effector cytokine IL-21 play an essential role in the occurrence and development of CRSwNP [19]. M2 macrophage has an anti-inflammatory effect. Loss of SENP3 will increase the number of M2 macrophages in the nasal mucosa, which is of great significance to CRS [20]. Studying the expression of different dendritic cells (DC) in patients with CRSwNP can be used as a critical measure in the progress of the disease [21]. Neutrophils have also been confirmed to be closely related to CRS pathology [22].

Finally, the interaction network between the hub genes and miRNA was constructed. So was the hub genes and TF. MiRNA can be used as a potential negative regulator of inflammation [23]. In the mouse experiment of CRS, Gu X et al. confirmed that the expression of mir-335–5p (the miRNA linked with NAIP and NLRC4) was related to CRS [24]. Morawska-Kochman M et al. found that there was no significant difference in the level of mir-146a-5p (miRNA linked with IL-18, NAIP, and NLRC4) between HC and CRSwNP, which may be due to the delayed induction of miR-146a/b, which may be a compensatory response to inhibit inflammation [25]. In Fig. 10B, we found that the protein encoded by MEF2A gene was involved in apoptosis. Previous studies have confirmed that apoptosis plays a vital role in the pathogenesis of CRS [11]. NR3C1 is involved in inflammatory reactions. Refractory rhinosinusitis (DTRS) is a particular type of CRS. Wu C et al. indicated that NR3C1 gene polymorphism is significantly related to DTRS [26]. EGR1 can regulate cell survival, proliferation, and cell death, activate the expression of p53/TP53 and TGFB1, and regulate the expression of a protein involved in the inflammatory process and tissue injury after ischemia, such as CXCL2 and IL1B. The level of CXCL2 is significantly correlated with the scope of CRS without nasal polyps (CRSsNP) disease [27]. Mfuna Endam L et al. studied the association between single nucleotide polymorphisms (SNP) in IL1B (rs16944) gene in CRS patients. Unfortunately, the association with IL1B has not been found, and further research is needed in the future [28].

This study used WGCNA and PPI analysis to identify targets and molecular pathways related to CRS. The biological significance of PRGs in CRS was explored at the genetic level through multiple data sets. In addition, ROC curve validation showed that the five hub genes highly predicted specificity and sensitivity. However, this study has some limitations that must be considered. First, the qRT-qPCR experiment only verified the expression difference of hub genes between CRSwNP samples and normal samples. The difference in expression between CRSSNP samples and normal samples was not confirmed. Secondly, there is no further experimental verification of the detailed molecular mechanisms of the five hub genes. In future studies, our research will focus on verifying the molecular functions and mechanisms of action of the five hub genes in CRS through biological experiments.

5. Conclusion

In a word, five hub genes were identified and verified by focusing on the role of apoptosis-related genes in CRS. In addition, the immune landscape of the hub genes in CRS and its interaction with miRNA and TF were discussed, respectively. In the future research,

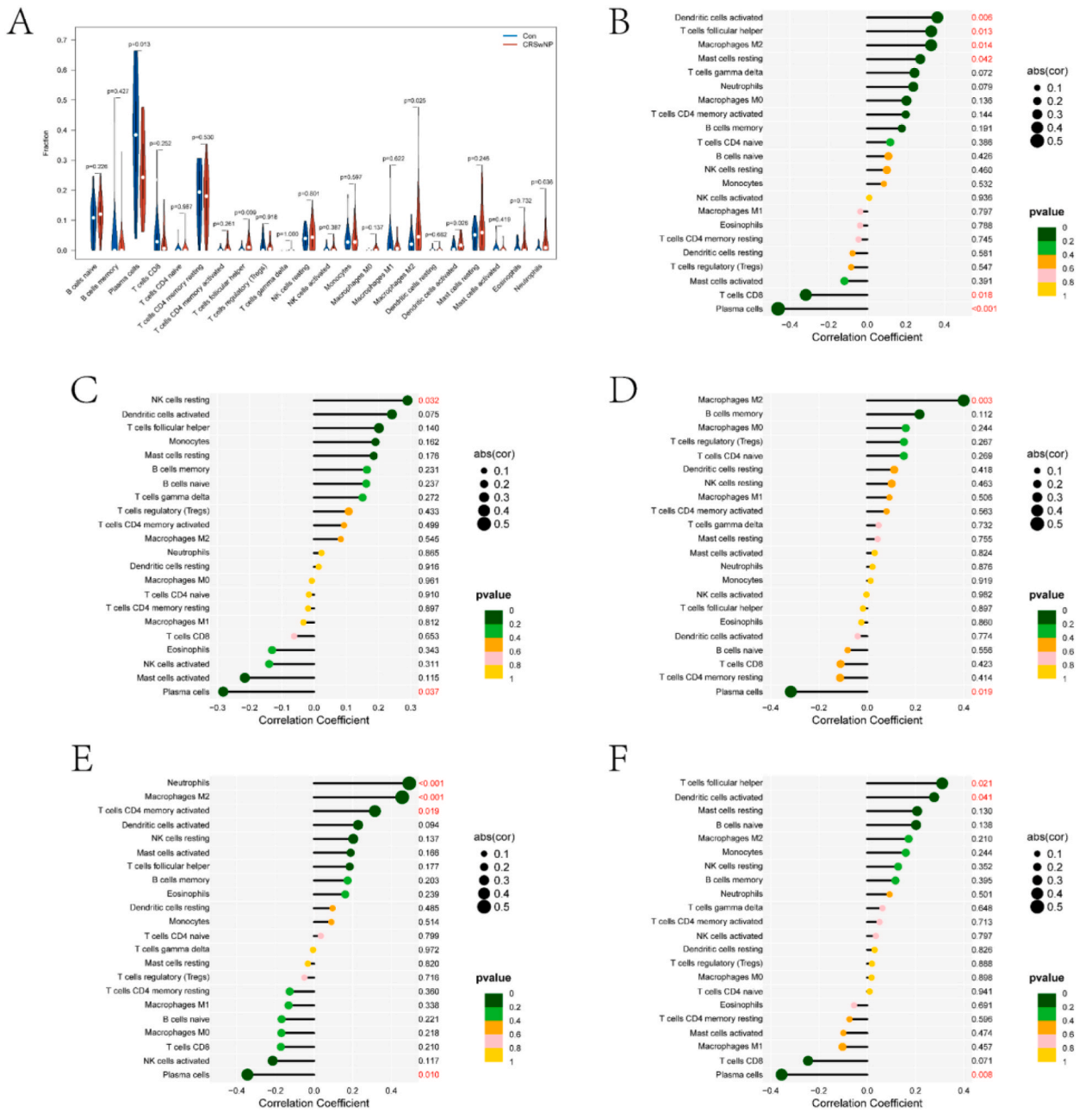

Fig. 10. CIBersort analysis based on hub genes. A is the difference in infiltration abundance of 22 kinds of immune cells in CRS and its control group. B–F are the bar graphs obtained from the correlation analysis between CASP3, IL18, NAIP, NLRC4, TP53, and immune cells.

we need to further verify these genes through experiments.

Ethics approval and consent to participate

Not applicable.

Consent for publication

Not applicable.

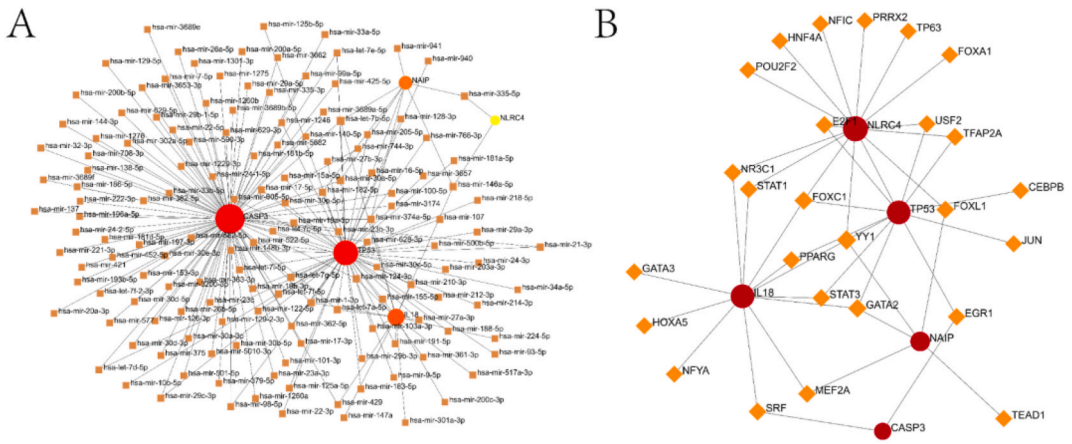

Fig. 11. The miRNA-TF interaction network of hub genes. A and B are the interaction networks of the hub genes, miRNA, and TF, respectively.

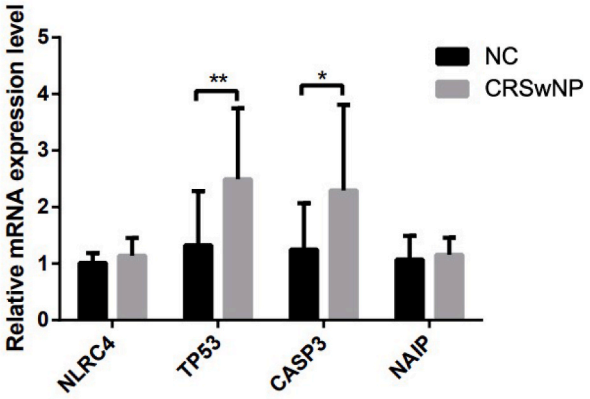

Fig. 12. The mRNA expression of NLRC4, TP53, CASP3 and NAIP in CRSwNP group and normal group was measured by qRT-qPCR. (*p < 0.05, **p < 0.01, * *P < 0.001).

Funding

Not applicable.

CRediT authorship contribution statement

Yarui Wan: Writing – original draft, Visualization, Methodology, Data curation. **Yanfei Wang:** Writing – original draft, Visualization, Software. **Sheng Xu:** Writing – review & editing, Resources, Methodology. **Hui Du:** Writing – review & editing, Supervision, Software. **Zhiqi Liu:** Writing – review & editing, Visualization, Supervision, Resources, Data curation.

Declaration of competing interest

The authors declare that they have no competing interests.

Data availability statement

The datasets analysed during the current study are available in the GEO database (https://www.ncbi.nlm.nih.gov/geo/). This article uses the GSE136825 dataset (https://www.ncbi.nlm.nih.gov/geo/query/acc.cgi?acc=GSE136825), the GSE179265 dataset (https://www.ncbi.nlm.nih.gov/geo/query/acc.cgi?acc=GSE179265), and the GSE36830 dataset (https://www.ncbi.nlm.nih.gov/geo/query/acc.cgi?acc=GSE36830).

Acknowledgements

Not applicable.

References

[1] J.B. Shi, et al., Epidemiology of chronic rhinosinusitis: results from a cross-sectional survey in seven Chinese cities, Allergy 70 (5) (2015) 533–539.
[2] R.P. Schleimer, Immunopathogenesis of chronic rhinosinusitis and nasal polyposis, Annu. Rev. Pathol. 12 (2017) 331–357.
[3] S.B. Kovacs, E.A. Miao, Gasdermins: effectors of pyroptosis, Trends Cell Biol. 27 (9) (2017) 673–684.
[4] R. Tang, et al., Ferroptosis, necroptosis, and pyroptosis in anticancer immunity, J. Hematol. Oncol. 13 (1) (2020) 110.
[5] P. Yu, et al., Pyroptosis: mechanisms and diseases, Signal Transduct. Targeted Ther. 6 (1) (2021) 128.
[6] S.K. Hsu, et al., Inflammation-related pyroptosis, a novel programmed cell death pathway, and its crosstalk with immune therapy in cancer treatment, Theranostics 11 (18) (2021) 8813–8835.
[7] Y. Li, et al., IL-17A mediates pyroptosis via the ERK pathway and contributes to steroid resistance in CRSwNP, J. Allergy Clin. Immunol. 150 (2) (2022) 337–351.
[8] Y. Yang, et al., Role of NLRP3 inflammasome on different phenotypes of chronic rhinosinusitis, Am J Rhinol Allergy 36 (5) (2022) 607–614.
[9] A. Nakatani, et al., S100A8 enhances IL-1β production from nasal epithelial cells in eosinophilic chronic rhinosinusitis, Allergol. Int. 72 (1) (2023) 143–150.
[10] S. Ding, et al., Prediction of the active components and possible targets of xanthii fructus based on network pharmacology for use in chronic rhinosinusitis, Evid Based Complement Alternat Med 2022 (2022), 4473231.
[11] M. Morawska-Kochman, et al., Expression of apoptosis-related biomarkers in inflamed nasal sinus epithelium of patients with chronic rhinosinusitis with nasal polyps (CRSwNP)-Evaluation at mRNA and miRNA levels, Biomedicines 10 (6) (2022).
[12] H.W. Yang, et al., Apigenin alleviates TGF-β1-induced nasal mucosa remodeling by inhibiting MAPK/NF-kB signaling pathways in chronic rhinosinusitis, PLoS One 13 (8) (2018), e0201595.
[13] J. Cheng, et al., MicroRNA-761 suppresses remodeling of nasal mucosa and epithelial-mesenchymal transition in mice with chronic rhinosinusitis through LCN2, Stem Cell Res. Ther. 11 (1) (2020) 151.
[14] H. Lin, et al., Expression and regulation of interleukin-9 in chronic rhinosinusitis, Am J Rhinol Allergy 29 (1) (2015) e18–e23.
[15] R.W. Liu, et al., [Expression and role of IL-18 in chronic rhinosinusitis], Lin Chuang Er Bi Yan Hou Tou Jing Wai Ke Za Zhi 32 (7) (2018) 497–501.
[16] J.S. Damiano, et al., Heterotypic interactions among NACHT domains: implications for regulation of innate immune responses, Biochem. J. 381 (Pt 1) (2004) 213–219.
[17] G.J. Huang, H.B. Liu, Identification and validation of ferroptosis-related genes for chronic rhinosinusitis with nasal polyps, Eur. Arch. Oto-Rhino-Laryngol. 280 (3) (2023) 1501–1508.
[18] H. Arjomandi, et al., Relationship of eosinophils and plasma cells to biofilm in chronic rhinosinusitis, Am J Rhinol Allergy 27 (4) (2013) e85–e90.
[19] L. Calus, et al., IL-21 is increased in nasal polyposis and after stimulation with Staphylococcus aureus enterotoxin B, Int. Arch. Allergy Immunol. 174 (3–4) (2017) 161–169.
[20] X. Bao, et al., Loss of SENP3 mediated the formation of nasal polyps in nasal mucosal inflammation by increasing alternative activated macrophage, Immun Inflamm Dis 11 (2) (2023) e781.
[21] R. Pezato, et al., The expression of dendritic cell subsets in severe chronic rhinosinusitis with nasal polyps is altered, Immunobiology 219 (9) (2014) 729–736.
[22] T. Delemarre, et al., Rethinking neutrophils and eosinophils in chronic rhinosinusitis, J. Allergy Clin. Immunol. 148 (2) (2021) 327–335.
[23] K.D. Taganov, et al., NF-kappaB-dependent induction of microRNA miR-146, an inhibitor targeted to signaling proteins of innate immune responses, Proc. Natl. Acad. Sci. U.S.A. 103 (33) (2006) 12481–12486.
[24] X. Gu, X. Yao, D. Liu, Up-regulation of microRNA-335-5p reduces inflammation via negative regulation of the TPX2-mediated AKT/GSK3β signaling pathway in a chronic rhinosinusitis mouse model, Cell. Signal. 70 (2020), 109596.
[25] D. Bhaumik, et al., MicroRNAs miR-146a/b negatively modulate the senescence-associated inflammatory mediators IL-6 and IL-8, Aging (Albany NY) 1 (4) (2009) 402–411.
[26] C. Wu, et al., The association between glucocorticoid receptor (NR3C1) gene polymorphism and difficult-to-treat rhinosinusitis, Eur. Arch. Oto-Rhino-Laryngol. 279 (8) (2022) 3981–3987.
[27] D.W. Kim, et al., Chronic rhinosinusitis without nasal polyps in asian patients shows mixed inflammatory patterns and neutrophil-related disease severity, Mediat. Inflamm. 2019 (2019), 7138643.
[28] L. Mfuna Endam, et al., Association of IL1A, IL1B, and TNF gene polymorphisms with chronic rhinosinusitis with and without nasal polyposis: a replication study, Arch. Otolaryngol. Head Neck Surg. 136 (2) (2010) 187–192.